Geophys. J. Int. (2001) **147,** 155–162

On the use of dislocations to model interseismic strain and stress build-up at intracontinental thrust faults

J. Vergne,[1] R. Cattin[2] and J. P. Avouac[1,2]

[1] *Laboratoire de Détection et de Géophysique,* B.P. 12, 91680 *Bruyénas-le-Châtes, CEA, France*
[2] *Laboratoire de Géologie, ENS,* 24 *Rue Llomond, Paris Cedex* 05, 75231, *France. E-mail: cattin@geologie.ens.fr*

Accepted 2001 May 23. Received 2001 March 8; in original form 2000 June 30

SUMMARY

Creeping dislocations in an elastic half-space are commonly used to model interseismic deformation at subduction zones, and might also apply to major intracontinental thrust faults such as the Main Himalayan Thrust. Here, we compare such models with a more realistic 2-D finite element model that accounts for the mechanical layering of the continental lithosphere and surface processes, and that was found to fit all available constraints on interseismic and long-term surface displacements. These can also be fitted satisfactorily from dislocation models. The conventional back-slip model, commonly used for subduction zones, may, however, lead to a biased inference about the geometry of the locked portion of the thrust fault. We therefore favour the use of a creeping buried dislocation that simulates the ductile shear zone in the lower crust. A limitation of dislocation models is that the mechanical response of the lithosphere to the growth of the topography by bending of the elastic cores and ductile flow in the lower crust cannot be easily introduced. Fortunately these effects can be neglected because we may assume, to first order, a stationary topography. Moreover, we show that not only can dislocation models be used to adjust surface displacements but, with some caution, they can also provide a physically sound rationale to interpret interseismic microseismicity in terms of stress variations.

Key words: continental deformation, dislocation, flexure of the lithosphere, seismotectonics.

1 INTRODUCTION

The theory of elastic dislocations (e.g. Okada 1992) is commonly used to model interseismic deformation near active faults; this deformation results from the elastic deformation of the brittle crust in response to plate displacement away from the fault zone and ductile shear at depth. For subduction zones, most authors rely on the seismic cycle model of Savage (1983) which considers two terms, namely a steady-state term equivalent to stable sliding along the whole thrust fault from the surface to its down-dip extension, and a cyclic term representing the stick-slip behaviour of the seismogenic portion of the fault (Fig. 1). In order to reproduce the locking of the seismogenic portion of the fault in the interseismic period, the cyclic term takes the form of a back-slipping elastic dislocation that compensates the steady-state term. If deformation due to the steady-state term is assumed to be negligible, interseismic straining is then simply modelled from the back-slip dislocation alone (Savage 1983). Although the validity of the assumption that no permanent deformation accumulates on the long term has been questioned (Matsu'ura & Sato 1989), this approximation has provided a satisfactorily fit to geodetic data in a number of subduction zones (e.g. Hydman & Wang 1995; Le Pichon *et al.* 1998; Savage *et al.* 2000). Gahalaut & Chander (1997) have proposed that this same rationale applies to intracontinental thrust faults, the best documented example being the major thrust fault at the front of the Himalaya (the Main Himalayan Thrust fault or MHT). In this case, the seismogenic portion of the thrust fault roots into a ductile shear zone in the lower crust. The hypothesis of localized slip along a thrust fault with prescribed slip rate and geometry may thus appear a crude and questionable approximation. In addition, some permanent deformation must also accumulate as the hanging wall slides along the flat–ramp–flat geometry of the MHT, and in response to loading by overthrusting and deposition in the foreland, and to unloading by erosion in the high range. Despite these potential limitations, some authors have used dislocation models to interpret geodetic data in the Himalaya. Gahalaut & Chander (1997) adopted the back-slip model, and later on introduced a steady-state term to account for accumulation of permanent deformation (Gahalaut & Chander 1999). This approach, then, is similar to modelling directly the creeping portion of the thrust fault at depth using a deeply buried dislocation, as done by several other authors (Bilham *et al.* 1997; Larson *et al.* 1999; Jouanne *et al.* 1999). All these approaches were found to provide a good fit to the measured horizontal and vertical displacements.

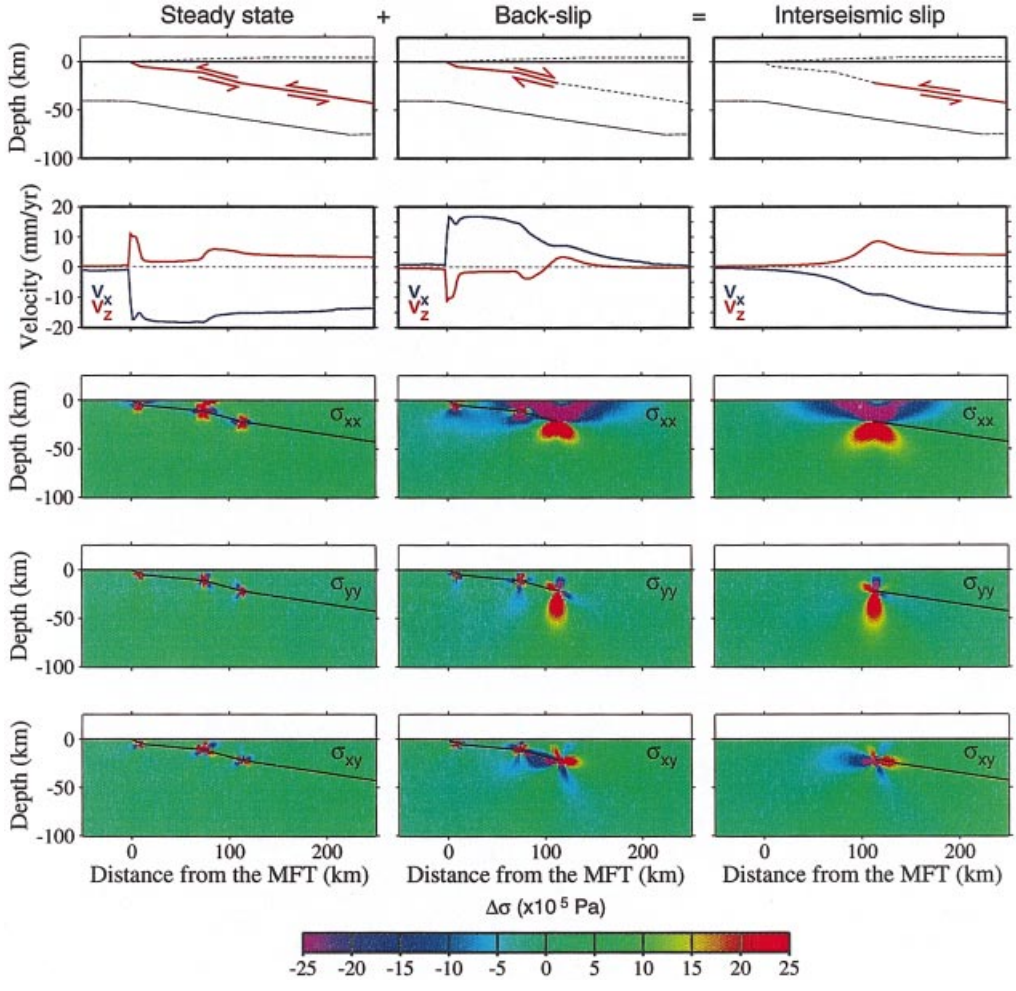

Figure 1. As for subduction zones (Savage 1983), interseismic deformation due to the locking of a major intracontinental thrust fault, such as the Main Himalayan Thrust fault, can be decomposed into two terms. The steady-state term expresses continuous slip along the fault and can be seen as some average over many seismic cycles. Note that it produces some permanent deformation of the hanging wall. The back-slip term counter-balances the steady motion on the locked portion of the fault. The fault geometry was derived from various geological and geophysical investigations (see discussion in Cattin & Avouac 2000). Surface displacements and the internal stress field were computed from the dislocation model of Okada (1992). X and Y are, respectively, the horizontal and the vertical components. X = 0 corresponds to the emergence of the MHT at the surface at the front of the sub-Himalayan foothills. V is the calculated velocity at the surface. V_X is positive in the northward direction. σ is the calculated stress field.

Recently, Cattin & Avouac (2000) investigated the relationship between microseismicity and stress build-up during the interseismic period along the MHT. This analysis required some computation of the variation of the stress field at depth. In view of the potential limitations of the dislocation models mentioned above, and because the use of dislocations is questionable for that purpose (Douglass & Buffet 1995; Savage 1996), we have preferred to use a 2-D finite element model that takes into account the rheological layering of the continental lithosphere, including in particular ductile flow in the lower crust, and erosion-sedimentation at the Earth's surface. We found that this model is indeed very sensitive to surface processes, and predicts a zone of Coulomb stress increase that coincides well with the observed cluster of seismicity. The model thus provides a single rationale to interpret quantitatively surface displacements and microseismicity. Along the same line, one may also want to investigate the significance of the lateral variations of both geodetic deformation and seismicity that are observed along the Himalaya of Nepal (Pandey *et al.* 1999; Larson *et al.* 1999; Jouanne *et al.* 1999). For that purpose, dislocation models will be much more convenient than finite element models, provided that they appear to be reasonable approximations for computing surface displacements as well as stress variations.

We therefore assess the validity of dislocation models to simulate interseismic straining at an intracontinental thrust fault in terms of both surface displacements and stress variation at depth. We show in particular that for stationary topography, counter-intuitively, it is better to ignore the mechanical response of the lithosphere to overthrusting, erosion and sedimentation when dislocation models are used.

2 THE REFERENCE MODEL

2.1 Geometry of the MHT and crustal deformation across the Himalaya of Nepal

The Himalaya of central Nepal are a case-example to investigate the mechanics of intracontinental thrust faulting (Fig. 2). The geometry of the Main Himalayan Thrust fault (MHT)

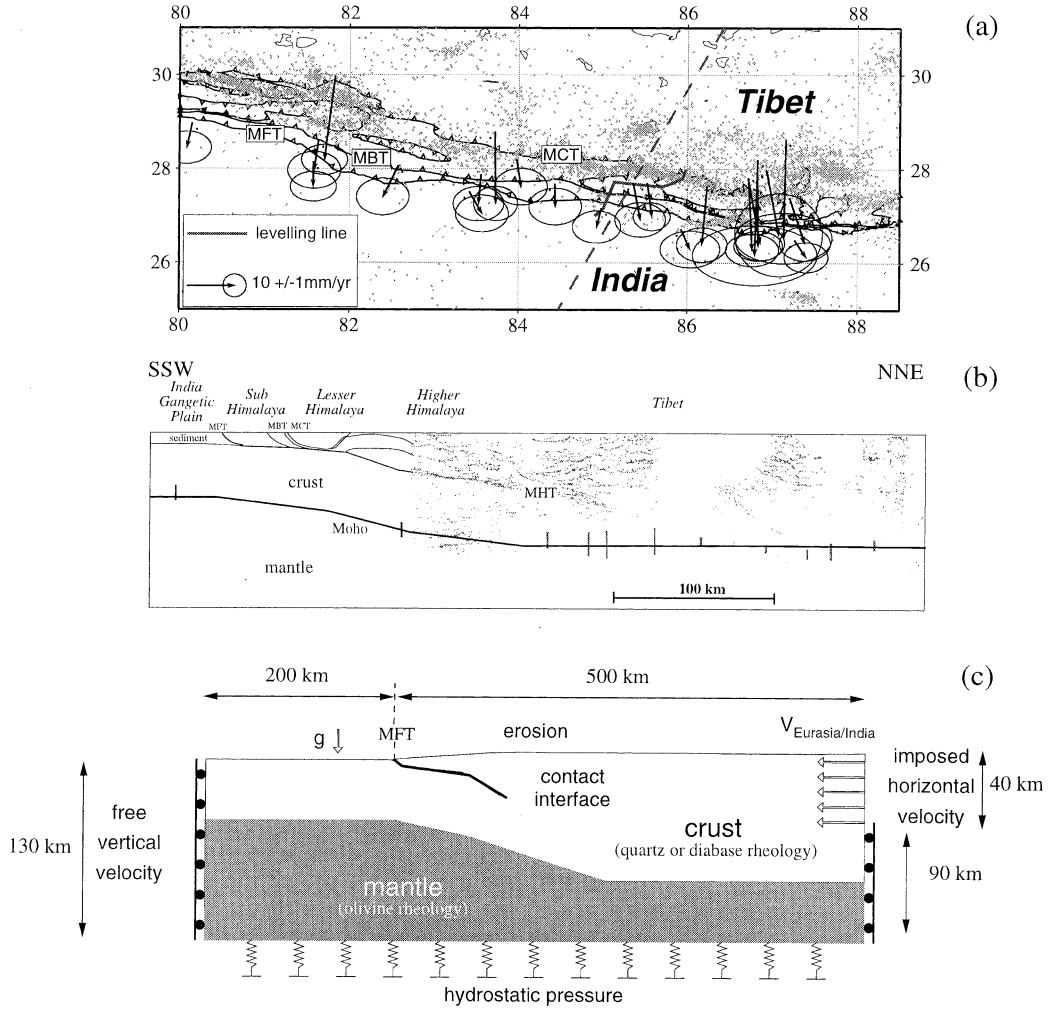

Figure 2. Geodynamic setting and description of the finite element model. (a) Seismotectonic map of the central Himalaya showing major structures (MFT: Main Frontal Thrust; MBT: Main Boundary Thrust; MCT: Main Central Thrust), geodetic measurements, and seismic data. GPS velocity vectors obtained by Larson *et al.* (1999) are represented with black arrows. Grey circles indicate microseismicity between 1994 and 1998 (Pandey *et al.* 1999). The black dashed line indicates the location of the N18°E cross-section discussed in this study. (b) Generalized cross-section across India, Nepal and Tibet derived from structural geology (Schelling & Arita 1991) and from seismic reflection profile and teleseismic receiver functions (Hauck *et al.* 1998; Saul *et al.* 2000). (c) The finite element model is submitted to 20 mm yr^{-1} of horizontal shortening. The model is loaded with gravitational body forces. Its base is supported by a hydrostatic foundation. Surface processes are simulated using a 1-D linear diffusion equation. The present mean topography along the profile is initially introduced. A depth-varying rheology is assumed to account for elasto-brittle and ductile deformation in the lithosphere. A fault with a simple Coulomb friction law is also introduced *a priori* to simulate the seismogenic zone, and follows the flat-and-ramp geometry proposed for the MHT in (b).

is relatively well known from geological and geophysical investigations in Nepal and southern Tibet (see Figs 2a and b). This fault emerges at the front of the foothills, makes a flat decollement under the Lesser Himalaya, and a mid-crustal ramp beneath the front of the Higher Himalaya. North of the high range, it probably roots into a subhorizontal shear zone that corresponds to the mid-crustal reflector, imaged at a depth of ~25 to ~40 km from seismic experiments (e.g. Nelson *et al.* 1996; Hauck *et al.* 1998) (Fig. 2b). The MHT can produce very large earthquakes such as the $M>8$ event that struck eastern Nepal in 1934. Over the two last decades, the interseismic strain across the range has been determined from GPS and levelling measurements (Bilham *et al.* 1997; Jackson & Bilham 1994; Larson *et al.* 1999; Jouanne *et al.* 1999) (Figs 2a and b). The long-term slip rate on the MHT is 21.5 ± 1.5 mm yr^{-1}, as indicated from the folding of dated fluvial terraces (Lavé & Avouac 2000) (Fig. 3).

2.2 The 2-D finite element model

In an attempt to reconcile the various data pertaining to the geometry of the MHT and deformation with the current understanding of the mechanics of the continental lithosphere, we used the 2-D finite element model ADELI (Hassani *et al.* 1997). The model accounts for crustal and mantle rheology, thermal structure of the lithosphere, geometry of the locked zone, topography, gravity, and erosion and sedimentation at the surface (see Cattin & Avouac 2000 for details).

We compute the thermal structure with the 2-D finite element model developed by Henry *et al.* (1997). The assumed boundary conditions are a constant surface temperature of 0°C, and a bottom heat flow of 15 mW m^{-2}. We use a relatively high heat production in the upper crust of 2.5 μW m^{-3}.The temperature-dependent rheology implies dominantly elasto-brittle deformation in the upper part of the crust, and ductile

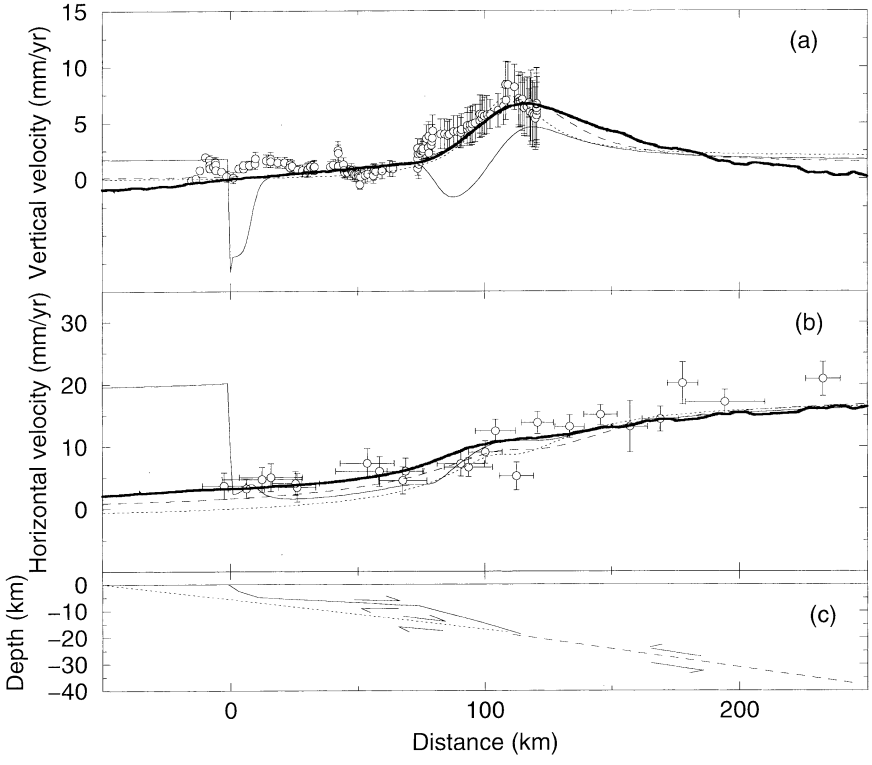

Figure 3. Comparison between measured and calculated interseismic velocities computed from the finite element model (thick line), the deeply buried creeping dislocation model (dashed line), the back-slip model (solid line), and the back-slip model proposed by Gahalaut & Chander (1997, 1999) (dotted line). (a) Vertical velocities relative to the southernmost point in the Indo-Gangetic plain, derived from levelling data (Jackson & Bilham 1994). (b) Horizontal velocities with respect to India derived from GPS measurements (Larson *et al.* 1999). (c) Fault geometry used in the dislocation model.

deformation in the lower part. We use an elastoplatic pressure-dependent law with the failure criterion of Drucker–Prager. A power-law creep simulates ductile flow in the lithosphere. For the upper mantle, an olivine-controlled rheology is assumed. For the crust we have used two end-members, by considering either a diabase-controlled rheology or a quartz-controlled rheology that favours decoupling between mantle and crust (see parameters in Cattin & Avouac 2000).

We consider a 700 km long section that approximates the N18°E section through the Himalaya of central Nepal (Fig. 2). The crustal thickness varies from 40 km beneath the Gangetic plain to 75 km beneath the Tibetan Plateau. At the southern and northern ends of the model, horizontal displacements are excluded and vertical displacements are free. The upper crust is submitted to 20 mm yr^{-1} of horizontal shortening. The model is loaded with gravitational body forces and is supported at its base by hydrostatic pressure to allow for the isostatic restoring force (Fig. 2c). We consider a flat and ramp system for the seismogenic portion of the MHT, which is assumed to be locked in the interseismic period. Steady-state slip is simulated using a low-friction coefficient to allow steady thrusting along the MHT. Following Avouac & Burov (1996), erosion is modelled from 1-D linear diffusion in the high range, and we assume flat deposition in the foreland.

This 2-D model does actually reconcile the available data on the MHT geometry and on deformation for the long term (over many seismic cycles) and during the interseismic period, but was found to be sensitive to surface processes. In particular, the model fits satisfactorily the vertical displacements derived from the levelling data as well as the horizontal displacements derived from GPS measurements (Fig. 3). A good adjustment can be obtained by assuming either a quartz (taken here to be our reference model) or a diabase rheology for the lower crust.

3 COMPARISON WITH DISLOCATION MODELS

3.1 The virtual back-slip dislocation model

As discussed above, the virtual back-slip model can be used if the secular deformation is small. The interseismic deformation is then calculated from a back-slip dislocation in a homogeneous elastic half-space. Gahalaut & Chander (1999) interpreted the levelling data using this model and found a relatively good fit by assuming a planar geometry for the MHT with a width of $\sim$150 km, a uniform dip angle of 6°, and a convergence rate of 20 ± 3 mm yr^{-1} (Fig. 3). This inferred geometry for the MHT is quite different from that obtained from geological and geomorphic investigations (Fig. 3).

If we now consider the geometry of the reference model described above and assume that the flat portion of the MHT and the ramp are locked, we cannot fit the data that well from the back-slip model (solid line in Fig. 3). The reason is that the steady-state term is not as simple as assumed by Gahalaut & Chander (1997) (Fig. 3); it has to account for the dip-angle

variations along the MHT (Fig. 2) and leads to deformations that cannot be neglected. This reveals the paradox of the back-slip model, in which interseismic displacements depend not only on the position of the lower end of the dislocation but also on the detailed geometry of the locked zone, which, by definition, should not have any influence on interseismic displacement. Thus, although the back-slip model may provide a relatively good fit to the geodetic data and a reasonable estimate of the slip rate on the MHT, it cannot be used to assess the geometry of the fault and might provide biased estimates of interseismic stress variations at depth.

3.2 Dislocation model of a buried fault associated with aseismic slip

If the steady-state term is added to the back-slip term, the model explicitly simulates aseismic creep beneath the high range and southern Tibet along the northward continuation of the seismogenic portion of the MHT. Gahalaut & Chander (1999) have investigated this, and considered that the steady-state term might be computed assuming that the hanging wall slips along the MHT and accommodates dip variations by vertical shear. Such a model predicts an uplift rate that is directly proportional to the sine of the dip angle of the MHT. In their model, this term is constant where the MHT has a uniform dip angle, so that this geometry does not affect the back-slip term, except at the emergence of the MHT where their model corrects for the abrupt step in the surface velocities (Fig. 3). Their model neglects any flexural response to overthrusting, erosion and sedimentation. A further shortcoming of this approach is that the steady-state term does not exactly balance the back-slip term because the two terms have different mechanical bases: ductile flow and elasto-brittle deformation over long time-scales (steady state), and elastic deformation without a failure criterion for the back-slip term. Therefore the stress variations cannot be reliably computed from such a model. The problem might be solved by computing the steady-state term from the elastic dislocation model as well. In that case the steady-state and the back-slip terms exactly compensate each other, so that we are left with a deeply buried dislocation that mimics ductile flow in the lower crust (Fig. 1). The problem now is that the steady state is computed from an elastic model that may allow for infinitely growing stresses due to dip variation along the MHT, which is incompatible with the rheology of the lithosphere (Fig. 1), and that the thickness of the shear zone in the lower crust is neglected. Most previous studies of interseismic deformation in the Himalaya were based on this approach (e.g. Jackson & Bilham 1994; Bilham *et al.* 1997; Larson *et al.* 1999; Jouanne *et al.* 1999; Gahalaut & Chander 1999).

Except where the fault emerges, the three approaches yield about the same horizontal velocities (Fig. 3). Unlike the back-slip model, the buried creeping dislocation also provides a good fit to the levelling data for a geometry of the MHT consistent with the one used in our reference model (Fig. 3). This model thus stands as the most convenient and realistic approximation to simulate surface displacements. It should be noted, however, that the back-slip model of Gahalaut & Chander (1997) also provides a correct fit to the horizontal velocities except where the MHT reaches the surface (Fig. 3). This shows that, for a perfectly locked seismogenic zone, the only meaningful parameters in the back-slip and buried-slip models are the position of the point at the deep end of the locked portion of the fault and the local dip angle of the zone of aseismic shear. The geometry of the back-slip dislocation does not need to follow that of the seismogenic portion of the fault.

3.3 Flexural response to erosion

Since vertical displacements in the interseismic period are very sensitive to surface processes (Cattin & Avouac 2000), we may be tempted to introduce this contribution to dislocation models together with the response to topographic changes. King *et al.* (1988) proposed a simple approach to do this. In the case of the Himalaya, the flexural response to overthrusting and erosion might not be that easy to compute because of the variations of effective flexural rigidity revealed from gravity modelling (Cattin *et al.* 2001).

Here, we first compute the mechanical response to erosion and sedimentation of the lithosphere using a thin elastic plate approximation. Following King *et al.* (1988), the effect of sedimentation and erosion is treated as a set of positive and negative loads acting on the top of the lithosphere. We then convolve the incision profile $V(x)$ with the deflection calculated from the expression for a line load at $x=0$:

$$w(x) = \frac{V(x=0)}{2\alpha\rho_{\mathrm{m}}g}\exp\left(\frac{-x}{\alpha}\right)\left[\cos(x/\alpha)+\sin(x/\alpha)\right],$$

where the flexural parameter is

$$\alpha = \left(\frac{4D}{\rho_{\mathrm{m}}g}\right)^{1/4},$$

and the flexural rigidity of the lithosphere is given by

$$D = \frac{Eh^3}{12(1-\nu^2)},$$

where E is Young's modulus, h is the elastic thickness of the lithosphere, ν is Poisson's ratio, and ρ_{m} is the mantle's density. The unloading profile is given by $V(x) = -\rho_{\mathrm{s}}ge(x)$, where $e(x)$ is the erosion rate deduced from river incision data (Lavé 1997), and ρ_{s} the density of sediments.

We have considered flexural rigidities between 10^{22} and 10^{25} N m, spanning the range of values obtained from gravity data analysis (Cattin *et al.* 2001). These studies have shown that the effective flexural rigidity is probably high beneath the Indo-Gangetic plain (10^{24}–10^{25} N m), and is much smaller (10^{23}–10^{24} N m) beneath the high range. These lateral variations are clearly of thermomechanical origin and are consistent with our finite element model, as discussed by Cattin *et al.* (2001). It turns out that, depending on the value of the flexural rigidity, the elastic response to erosion should contribute 1.5–3 mm yr^{-1} of uplift in the high range relative to the north of the Gangetic plain. We have compared these simulations with the flexural response of our 2-D finite element model as derived from a specific experiment. In this experiment, the lithosphere is submitted to horizontal shortening but surface processes are not considered initially. The onset of the erosion profile is introduced suddenly so that the pattern of uplift changes abruptly (the thick line in Fig. 4 shows the difference in the uplift pattern before and after erosion). In doing this, we have isolated the instantaneous response of the lithosphere to erosion and sedimentation without allowing for a feed-back effect on the lower crustal flow.

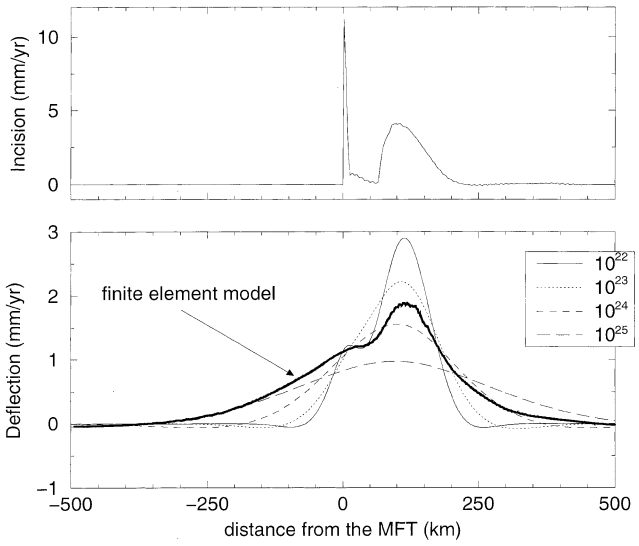

Figure 4. Surface uplift due to the flexural response of the lithosphere to erosion. The denudation-rate profile is given in (a) (from Lavé 1997). The flexural response was calculated from a thin elastic plate approximation with a flexural rigidity between 10^{22} and 10^{25} N m, and from the 2-D finite element model. See details in text.

A comparison of this simulation with the analytical solutions obtained from the thin-plate approximation also shows the lateral variations inferred from the gravity modelling. The smooth pattern in the foreland reflects an effective flexural rigidity of the order of 10^{25} N m, much higher than beneath the high range where our model predicts a narrow peak more consistent with a value between 10^{23} and 10^{24} N m. More importantly, this comparison shows that the flexural response to denudation (and also to tectonic uplift) cannot be approximated from simple elastic plate models. Another problem arises from the fact that ductile flow in the lower crust is coupled with surface processes (Avouac & Burov 1996), so that neither of these terms should be considered independently. Fortunately, on average over the long term and at the scale of an orogeny, this coupling leads to a balance between tectonic uplift and denudation (Cattin & Avouac 2000).

It thus turns out that, in order to simulate interseismic deformation using dislocation models, it is better not to introduce any of these terms and to assume that the topography is stationary. This is only a crude approximation, but the most appropriate for the model to remain simple. It should be noted, however, that such an assumption might not hold in other contexts.

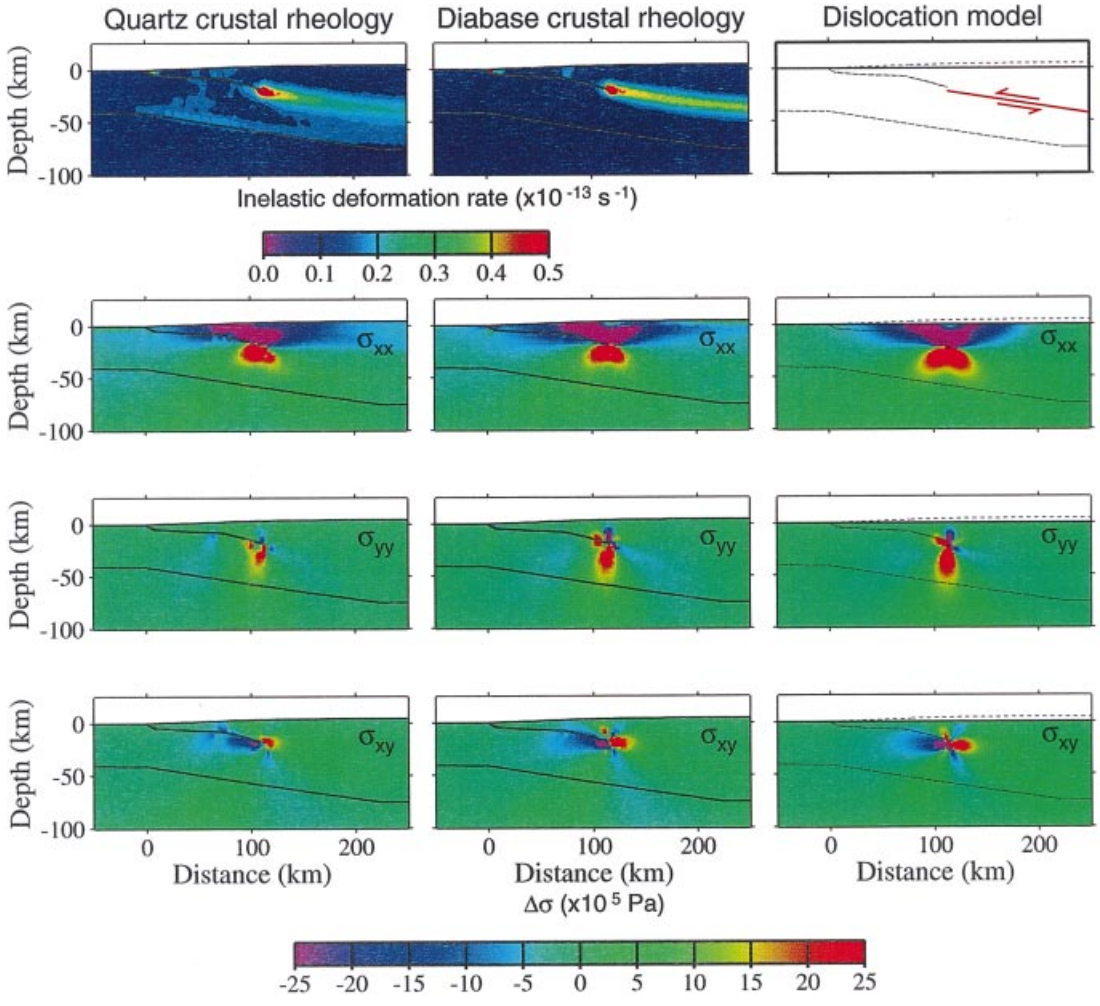

Figure 5. Comparison of the interseismic stress field computed from the buried-slip model and from the finite element model. The quartz-like rheology implies a relatively thin elastic core in the middle crust and a thick ductile shear zone in the lower crust. The diabase rheology results in a stronger crust with more localized ductile shear in the lower crust.

4 COMPUTING INTERSEISMIC STRESS VARIATIONS FROM A DISLOCATION MODEL

In this section, we demonstrate the validity of dislocation models to compute interseismic stress build-up at the MHT. We compute the stress-rate field from the buried dislocation model and compare it with the results of two finite element models, which consider either a quartz-like (our reference model) or a diabase-like rheology for the lower crust. These two rheologies might indeed be considered as end-members (see discussion in Cattin & Avouac 2000). The diabase rheology predicts a much narrower shear zone than our reference model, and is thus closer to the approximation of a velocity discontinuity (Fig. 5). A comparison with the stress-rate field computed from the buried dislocation model shows only minor differences, meaning that the thickness of the shear zone has little effect on the stress field at the scale of the crust. Apart from the large differences in peak values at the leading edge of the dislocation, the major difference lies in the lower crust. In the finite element models, stress increase at the edge of the shear zone is partly relaxed by ductile flow. It follows that the lobes in the lower crust do not grow as rapidly as in the creeping buried dislocation model. We thus recommend caution as to the interpretation of stress variation in the lower crust computed from dislocation models. This approach can be used to compute the stress field variation in the upper crust and to discuss the correlation of the zone of Coulomb stress increase with microseismicity in the interseismic period (Fig. 6).

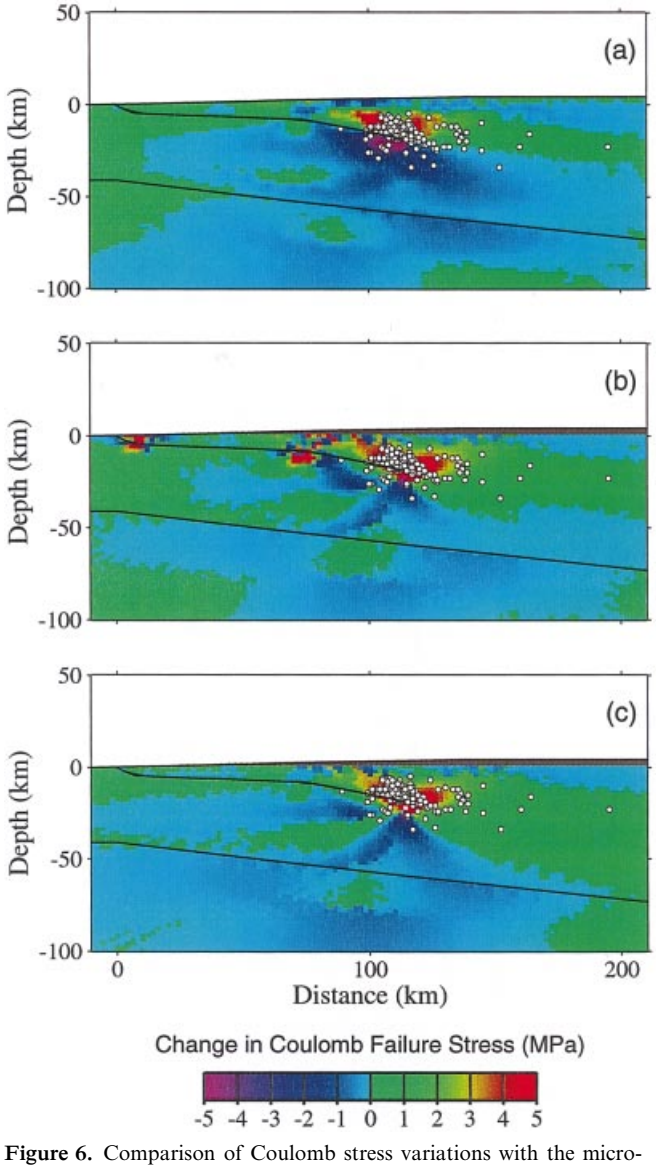

Figure 6. Comparison of Coulomb stress variations with the microseismic activity recorded in central Nepal (Cattin & Avouac 2000). Coulomb stress variations were computed from the finite element reference model (a), the back-slip model of Gahalaut & Chander (1997, 1999) (b), and the buried-slip model (Bilham *et al.* 1997; Jouanne *et al.* 1999; Larson *et al.* 1999) (c). All three models can be used to analyse jointly seismicity data and surface deformation.

5 CONCLUSIONS

Our study shows that, as along subduction zones, dislocation models can be used to model interseismic surface deformation near major intracontinental thrust faults. We show that, when such simplified models are used, it is better not to account for the mechanical response of the lithosphere to erosion and sedimentation. This is because, in the Himalayan context, tectonic uplift and denudation tend to balance each other due to the coupling between surface processes and ductile flow in the lower crust. Contrary to Douglass & Buffet (1995), we find that the stress field variations can also be computed satisfactorily from this approach, provided that the model is used over a time span consistent with the characteristic duration of interseismic periods. Such a modelling might therefore provide a physically sound basis for the joint interpretation of geodetic and microseismicity data pertaining to interseismic strain and stress accumulation near major thrust faults. Either buried creeping dislocation or back-slip dislocation can be used, but it should be noted that the geometry of the back-slip dislocation may have no bearing on the real geometry of the seismogenic fault. Although it constitutes a convenient model for subduction zones, where measurements are generally confined to the hanging wall and relatively far away from the trench, the back-slip model might be somewhat misleading.

ACKNOWLEDGMENTS

We thank K. Regenauer-Lieb and J. C. Savage for their thoughtful comments. We are grateful to Y. Okdada for providing his Fortran routines from his 1992 paper and to J. Chéry for the finite element code ADELI.

REFERENCES

Avouac, J.P. & Burov, E.B., 1996. Erosion as a driving mechanism of intracontinental mountain growth, *J. geophys. Res.,* **101,** 17 747–17 769.

Bilham, R., Larson, K., Freymueller, J. & Project Idylhim members, 1997. GPS measurements of present-day convergence across the Nepal Himalaya, *Nature,* **386,** 61–64.

Cattin, R. & Avouac, J.P., 2000. Modeling mountain building and the seismic cycle in the Himalaya of Nepal, *J. geophys. Res.,* **105,** 13 389–13 407.

Cattin, R., Martelet, G., Henry, P., Avouac, J.P. & Diament, M. & Shakya, T.R., 2001. Gravity anomalies, crustal structure and thermomechanical suuport of the Himalayas of Central Nepal, *Geophys. J. Int.,* in press.

Douglass, J.J. & Buffet, B.A., 1995. The stress state implied by dislocation models of subduction deformation, *Geophys. Res. Lett.,* **22,** 3115–3118.

Gahalaut, V.K. & Chander, R., 1997. On interseismic elevation changes for great thrust earthquakes in the Nepal Himalaya, *Geophys. Res. Lett.,* **24,** 1011–1014.

Gahalaut, V.K. & Chander, R., 1999. On interseismic elevation changes observed near 75.5°E longitude in the NW Himalaya, *Bull. seism. Soc. Am.,* **89,** 837–843.

Hassani, R., Jongmans, D. & Chéry, J., 1997. Study of plate deformation and stress in subduction processes using two-dimensional numerical models, *J. geophys. Res.,* **102,** 17 951–17 965.

Hauck, M.L., Nelson, K.D., Brown, L.D., Zhao, W. & Ross, A.R., 1998. Crustal structure of the Himalayan orogen at $\sim 90^{\circ}$ east longitude from Project INDEPTH deep reflection profiles, *Tectonics,* **17,** 481–500.

Henry, P., Le Pichon, X. & Goffé, B., 1997. Kinematic, thermal and petrological model of the Himalayas: constraints related to metamorphism within the underthrust Indian crust and topographic elevation, *Tectonophysics,* **273,** 31–56.

Hyndman, R.D. & Wang, K., 1995. The rupture zone of Cascadia great earthquakes from current deformation and the thermal regime, *J. geophys. Res.,* **100,** 22 133–22 154.

Jackson, M. & Bilham, R., 1994. Constraints on Himalaya deformation inferred from vertical velocity fields in Nepal and Tibet, *J. geophys. Res.,* **99,** 13 897–13 912.

Jouanne, F. *et al.*, 1999. Oblique convergence in the Himalayas of western Nepal deduced from preliminary results of GPS measurements, *Geophys. Res. Lett.,* **26,** 1933–1936.

King, G.C.P., Stein, R.S. & Rundle, J.B., 1988. The growth of geological structures by repeated earthquakes, 1. Conceptual framework, *J. geophys. Res.,* **93,** 13 307–13 318.

Larson, K., Bürgmann, R., Bilham, R. & Freymueller, J.T., 1999. Kinematics of the India-Eurasia collision zone from GPS measurements, *J. geophys. Res.,* **104,** 1077–1093.

Lavé, J., 1997. Tectonique et érosion, L'apport de la dynamique fluviale à l'étude sismotectonique de l'Himalaya du Népal central, *PhD thesis,* Université Paris 7, Paris.

Lavé, J. & Avouac, J.P., 2000. Active folding of fluvial terraces across the Siwaliks Hills, Himalayas of central Nepal, *J. geophys. Res.,* **105,** 5735–5770.

Le Pichon, X., Mazzotti, S., Henry, P. & Hashimoto, M., 1998. Deformation of the Japanese Islands and seismic coupling: an interpretation based on GSI permanent GPS observations, *Geophys. J. Int.,* **134,** 501–514.

Matsu'ura, M. & Sato, T., 1989. A dislocation model for the earthquake cycle at convergent plate boundaries, *Geophys. J.,* **96,** 23–32.

Nelson, K.O. *et al.*, 1996. Partially molten middle crust beneath southern Tibet, synthesis of project INDEPTH results, *Science,* **274,** 1684–1688.

Okada, Y., 1992. Internal deformation due to shear and tensile faults in a half space, *Bull. seism. Soc. Am.,* **82,** 1018–1040.

Pandey, M.R., Tandukar, R.P., Avouac, J.P., Vergne, J. & Héritier, J.P., 1999. Seismotectonics of the Nepal Himalaya from a local seismic network, *J. Asian Earth. Sci.,* **17,** 703–712.

Saul, J., Kumar, M.R. & Sarkar, D., 2000. Lithospheric and upper mantle structure of the Indian Shield, from teleseismic receiver functions, *Geophys. Res. Lett.,* **27,** 2357–2360.

Savage, J.C., 1983. A dislocation model of strain accumulation and release at a subduction zone, *J. geophys. Res.,* **88,** 4984–4996.

Savage, J.C., 1996. Comment on 'The stress state implied by dislocation models of subduction deformation' by Douglass and Buffet, *Geophys. Res. Lett.,* **23,** 2709–2710.

Savage, J.C., Svarc, J.L., Prescott, W.H. & Murray, M.H., 2000. Deformation across the forearc of the Cascadia subduction zone at Cape Blanco, Oregon, *J. geophys. Res.,* **105,** 3095–3102.

Schelling, D. & Anita, K., 1991. Thrusts tectonics, crustal shortening and the structure of the Far Eastern Nepal Himalaya, *Tectonics,* **10,** 851–862.